Investigation of the heteroepitaxial interfaces in the GaInP/GaAs superlattices by high-resolution x-ray diffractions and dynamical simulations

Cite as: Journal of Applied Physics **73**, 3284 (1993); https://doi.org/10.1063/1.354038
Submitted: 24 September 1992 . Accepted: 15 December 1992 . Published Online: 04 June 1998

Xiaoguang He, and Manijeh Razeghi

Investigation of the heteroepitaxial interfaces in the GaInP/GaAs superlattices by high-resolution x-ray diffractions and dynamical simulations

Xiaoguang He and Manijeh Razeghi
Center for Quantum Devices, Department of Electrical Engineering and Computer Science, Northwestern University, Evanston, Illinois 60208

(Received 24 September 1992; accepted for publication 15 December 1992)

Two GaAs/GaInP superlattices grown on GaAs substrates by low-pressure metalorganic chemical vapor deposition have been studied using high resolution x-ray diffraction measurements and simulations by solving Tagaki–Taupin equations. The strained layers at both interfaces of the GaAs well are identified from the simulations of the measured diffraction patterns. The purging of indium at the interface of GaInP/GaAs accounts for the strained layer at the GaInP/GaAs interface while the pressure difference in the gas lines, which results in the different traveling time to the sample surface, is attributed to the indium-poor strained layer at the GaAs/GaInP interface. It is shown that high-resolution x-ray diffraction measurements combined with a dynamical simulation, are sensitive tools to study the heteroepitaxial interfaces on an atomic layer scale. In addition, the influence of a miscut of the substrate on the measurement is discussed in the article. It is shown that even though the miscut is small, the diffraction geometry is already an asymmetric one. More than 10% error in the superlattice period for a 2° miscut substrate can result when the miscut substrate is considered a symmetric geometry.

I. INTRODUCTION

The continued progress in the epitaxial growth techniques has made possible the fabrication of semiconductor heterostructures with a large degree of crystalline perfection. This, in turn, has led to more in-depth structural studies of heterostructures. Superlattices, which have a large number of heteroepitaxial interfaces and have many x-ray interference fringes due to a large superlattice period, have increasingly become the focus of structural analysis.[1] There have been various high-resolution x-ray diffraction (HRXRD) characterizations on such superlattices.[1–4] Combined with the x-ray dynamical simulation, detailed information up to the atomic layer scale is acquired by the HRXRD technique, the accuracy of which is confirmed by the high-resolution transmission electronic microscope (HRTEM).

High-quality GaAs/GaInP heterojunctions have been successfully grown by low-pressure metalorganic chemical vapor deposition (LP-MOCVD) and characterized by various techniques.[5–7] Yet, the interfacial strain is not well understood for these samples. It has been suggested that interfacial strain can affect the band offset of the heterojunction and the performance of the devices.[8] Obviously, the understanding of the strain at the interfaces and the origin of these strains is imperative to the improvement of the material growth and device fabrication.

In this article, studies on two GaAs/GaInP superlattice samples grown by LP-MOCVD are presented using high-resolution x-ray diffraction measurements and simulations based on the dynamic x-ray diffraction theory.[9] The evidence of the strained layers at both GaAs/GaInP and GaInP/GaAs interfaces is demonstrated through a simulation of the measured diffraction patterns and the origin of these strains is discussed. Also in this article, the influence of the miscut of the substrate, which is common for almost all epitaxial samples, is discussed.

II. THEORETICAL BACKGROUND

The angular separation $\Delta\theta$ between the diffraction peak of substrate and that of the epilayers enables us to determine the mismatch and, as a result, the alloy composition of the epilayers by Vegard's law. The lattice parameter a of a substance with a cubic structure is directly proportional to the spacing d of any particular set of lattice planes, which is measured in the x-ray diffraction experiment. The angular separation between Bragg's peaks can be related to the lattice mismatch through the differential form of the Bragg's law[9]

$$(\Delta a/a_0)_{\text{perp}} = -\cot\theta_B \Delta\theta, \tag{1}$$

where θ_B is the Bragg angle of substrate and a_0 is the lattice constant of substrate. $(\Delta a/a_0)_{\text{perp}}$ represents the lattice strain perpendicular to the crystal surface, which is related to the relaxed lattice mismatch $(\Delta a/a_0)_r$ by[9]

$$(\Delta a/a_0)_r = (\Delta a/a_0)_{\text{perp}}[C_{11}/(C_{11}+2C_{12})], \tag{2}$$

provided that the in-plane strain $(\Delta a/a_0)_{\text{para}}$ is assumed to be zero, or that the lattice constant parallel to the substrate surface remains the same as that of substrate. C_{ij} is the elastic stiffness constant for the layer material. From this relaxed mismatch, the relaxed lattice constants of the epilayer is obtained. As a result, the mole fraction of the ternary epilayer can be determined by Vegard's law.

In addition to the Bragg diffraction peaks, the interference fringes from a well-defined crystalline shape are displayed in the x-ray diffraction experiments. These interfer-

 0021-8979/93/073284-07$06.00

ence fringes, arising from the interaction among the x-rays reflected from each layer of the samples, convolute with the Bragg diffraction peaks to show us the total diffraction pattern. The intensities and separations of interference fringes are related to the thicknesses of the layers, the structure factors of the constitute materials and the interface roughness. The relation between the angular separation of the interference fringes and the thickness of the layer, D, at the symmetric geometry is

$$D=\lambda/2\Delta\theta\cos\theta_B, \tag{3}$$

where λ is the wavelength of the x ray. $\Delta\theta$ is the separation of the neighboring peaks and θ_B is the Bragg peak of the epilayer. In the case of a multilayer structure, harmonics from various combinations of the constituent layers contribute to the diffraction pattern, which becomes difficult to analyze. A simulation based on dynamic x-ray diffraction theory has to be used to analyze the possible thicknesses of the each constituent layer. In this work, we simulated the observed diffraction patterns by solving Tagaki–Taupin equations.[10,11] The fitting is acquired by a trial-and-error method.

Superlattices, as a special case of a multilayer structure that is the periodic repetition of a superlattice unit cell, give rise to intensified and sharpened peaks due to its periodic structure. In this case, the diffraction pattern displays several sharp peaks, with the angular separation being proportional to the reciprocal of the superlattice period. These peaks are usually called superlattice satellites. The intensities of the superlattice satellites are modulated by the harmonics of the individual layers that constitute the superlattice unit cell.

III. EXPERIMENTS

The two samples studied here are ten-period GaAs/GaInP superlattices grown by LP-MOCVD on GaAs (001) substrates misoriented 2° off towards $\langle\bar{1}10\rangle$ (miscut 2°). The nominal well thicknesses and barrier thicknesses are 90 and 600 Å for sample I and 90 and 100 Å for sample II, respectively. All epilayers were nominally undoped. Residual impurity concentrations are assumed to be of the order of those determined for bulk layers. Corresponding layers of GaAs and GaInP with thicknesses of 3 μm, grown under identical conditions, revealed N_D-$N_A\leqslant 10^{14}$ cm^{-3} for GaAs (Ref. 12) and N_D-$N_A\leqslant 5\times 10^{14}$ cm^{-3} for GaInP (Ref. 13) and showed that a uniform distribution of impurities in the direction perpendicular to the layers has been obtained. The flow sequence of the sources is shown in Fig. 1 and the growth conditions were published in an earlier article.[7]

A four-crystal monochromator x-ray diffractometer (MPD1880/HP),[14] developed at Philips Research Laboratories, is used to measure diffraction patterns. The monochromator in the machine is composed of two "U"-shaped blocks of highly perfect germanium. Ge (220) is used as the monochromator plane in this work. The full width at half-maximum (FWHM) of the beam under this setting is 12 s.

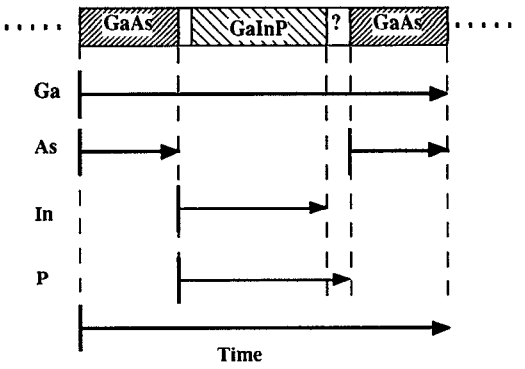

FIG. 1. The flow sequence of the sources during the growth of GaInP/GaAs superlattices.

(004) and (002) diffractions are measured to study the structural parameters of the samples. (004) diffraction is the most commonly studied diffraction for $\langle 001\rangle$ oriented III-V semiconductors, being the point where all atomic planes within the sample scatter in phase. Hence, (004) diffraction will be the most intense, and will exhibit features from the whole sample structure. For the samples containing GaAs, (002) diffraction is more revealing, because the structure factor of GaAs (002) diffraction is much smaller than that of GaInP. Thus, (002) diffraction exhibits features predominantly from the GaInP. All of the diffractions are measured at a θ-2θ mode with a fine collimating of the incident and diffracted x rays in order to track the evolution of the superlattice harmonics over several degrees. The more usual rocking curve measurements could not be employed for the (002) or (004) reflections due to the large angular extent of superlattice satellites.

It was found that the measured diffraction patterns depend on the orientation of the miscut of the samples relative to the x-ray beam plane. In this work, (002) and (004) diffraction patterns are acquired by adjusting the miscut edge parallel to the x-ray beam plane at $\varphi=90°$, which is shown in the schematic drawing of the geometry of x-ray diffraction in Fig. 2; in this direction, diffraction patterns are independent of the miscut value. Asymmetric geometry (115) reflections are measured at two setting with 180° difference in azimuthal angle φ around $\langle 001\rangle$ of the substrate to determine the tilt of the epilayers. The tilt of the sample may affect the measurement of mismatch from the diffraction pattern. Fortunately, the tilt of two samples in this work is in the same direction as the miscut. This is known to be the case because the mismatches, measured at two azimuthal angles that have the miscut edge parallel to the beam plane ($\varphi=90°$), are the same within the measurement tolerance. Thus, no tilt effect needs to be considered in the measurement of the mismatch and in the simulations of diffraction patterns.

IV. RESULTS AND DISCUSSION

A. Effect of substrate miscut to the measured superlattice period

The miscut substrate has been widely used in the crystal growth. The reason is that a miscut surface provides a

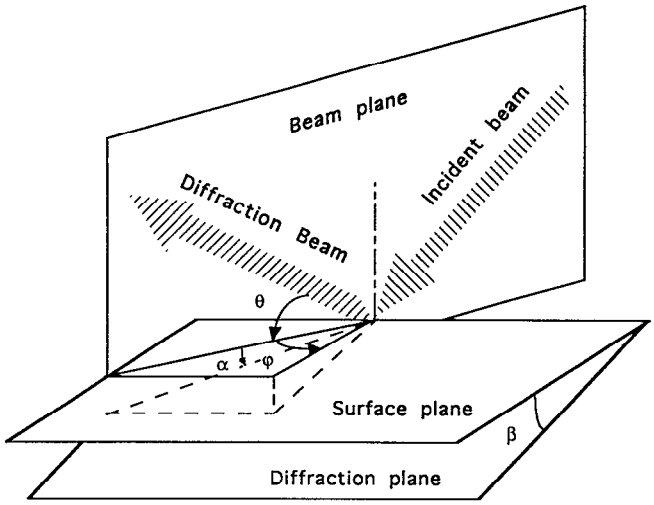

FIG. 2. Schematic drawing of the geometry of x-ray diffraction.

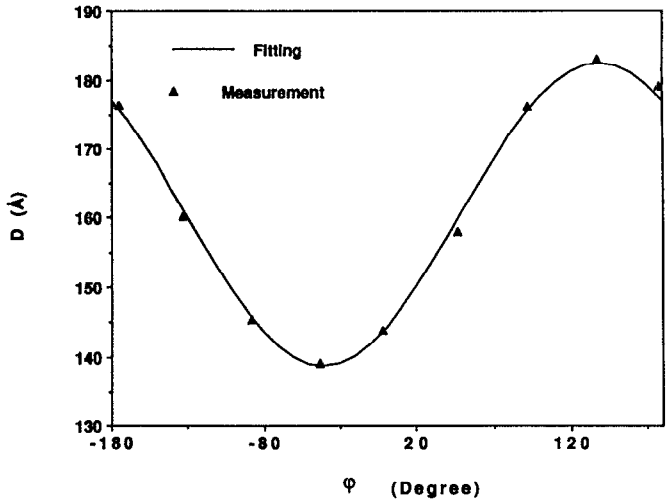

FIG. 3. The relation between measured suplattice periods of sample II by Eq. (3) and the azimuthal angle φ.

step, which results in easier growth, and thus gives better interfacial quality. The effect of the miscut of the substrate on the measurement result was found when it was noticed that there is about 5% difference in the measured superlattice period between (002) diffraction and (004) diffractions according to Eq. (3). This error is impossible for a precise measurement like HRXRD. The origin of observed discrepancy is that Eq. (3) is only valid for symmetric geometry. For the miscut substrate, the diffraction is from an asymmetric geometry. The real thickness D_{asym} is given by

$$D_{\text{asym}}=\lambda \sin(\theta_B+\alpha)/\Delta\theta \sin(2\theta_B), \tag{4}$$

when the separation of the neighboring peaks, $\Delta\theta$, is not too large and where θ_B is the Bragg diffraction angle of the epilayers and α is the cross section angle in the beam plane between the diffraction plane and the surface plane as in Fig. 2. A relation among α, miscut β, and azimuthal angle φ can be obtained from Fig. 2 as

$$\tan\alpha=\tan\beta\cos\varphi. \tag{5}$$

Combining Eqs. (4) and (5) under the limit that miscut β is small, we have the relation between the real superlattice period D_{asym} and the period D calculated from Eq. (3):

$$D_{\text{asym}}=D(1+\beta\cot\theta_B\cos\varphi). \tag{6}$$

When $\beta\cot\theta \ll 1$, Eq. (6) can be approximated as

$$D=D_{\text{asym}}(1-\beta\cot\theta_B\cos\varphi). \tag{7}$$

Figure 3 shows that a satisfactory agreement of D with Eq. (7) is obtained. β and D_{asym} from the fitting are 2.2° and 160 Å, respectively. This miscut value is close to the nominal value (2°) and the superlattice period obtained is also close to the thickness measured from a HRTEM picture (to be published elsewhere).

B. Diffraction patterns and simulations

All the diffraction patterns presented here have considered the influence of the substrate miscut and the tilt of the epilayers by deliberately adjusting the azimuthal angle φ in Fig. 2.

Figure 4(a) shows the (002) diffraction pattern of sample 1. The sharp peaks, a typical shape of the superlattice satellites, up to 18th order with 6 modulations of the superlattice satellites due to the large superlattice unit cell are observed. The superlattice period corresponding to the observed separation of the superlattice satellites is 612±4 Å according to Eq. (3). The observed modulation of the superlattice satellites may arise from the GaAs well. Fine fringes around the central order superlattice satellite indicate a layer with a thickness of 6519±304 Å, which may be associated with the total epilayer, because this thickness is consistent with the fact that the sample is a ten-period superlattice (11 barriers). No apparent mismatch is observed in the (002) pattern. Since the 0th order superlattice satellite overlaps with the substrate peak, the diffraction pattern should be completely symmetric around the 0th order peak. The strong asymmetry observed definitely indicates the existence of the interfacial layer in the superlattice unit cell.

Figure 5(a) shows the (004) diffraction pattern for sample I. Superlattice satellites up to 16th order with 6 modulations due to the large superlattice unit cell are observed. The superlattice period corresponding to the observed separation of the superlattice satellites is 616±5 Å. The modulation of the superlattice satellite is less intense than that in (002). Some fine structure at the superlattice satellite peaks, which are more clear for the minus order satellite, indicates the existence of the gradient of the mismatch through the superlattice unit cell.[15] No clear fringe corresponding to the total epilayer is observed. A relaxed mismatch of −0.019% is derived from the separation of the substrate peak from the 0th order superlattice satellite in (004) diffraction pattern.

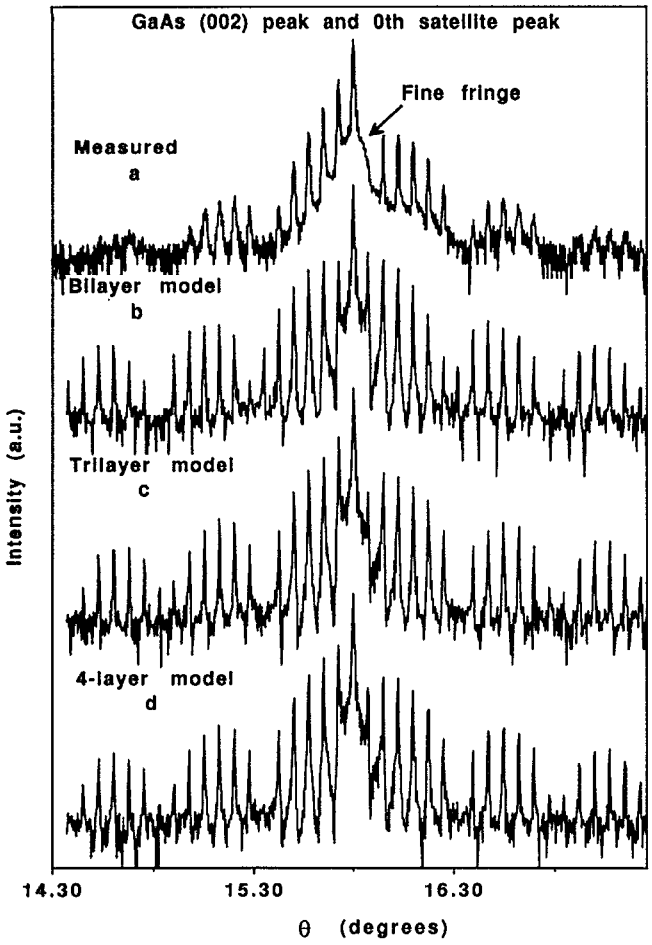

FIG. 4. (002) diffraction patterns of sample I from measurement and simulations; (a) measured pattern, (b) simulated pattern with the bilayer model, (c) simulated pattern with the trilayer model, and (d) simulated pattern with the four-layer model.

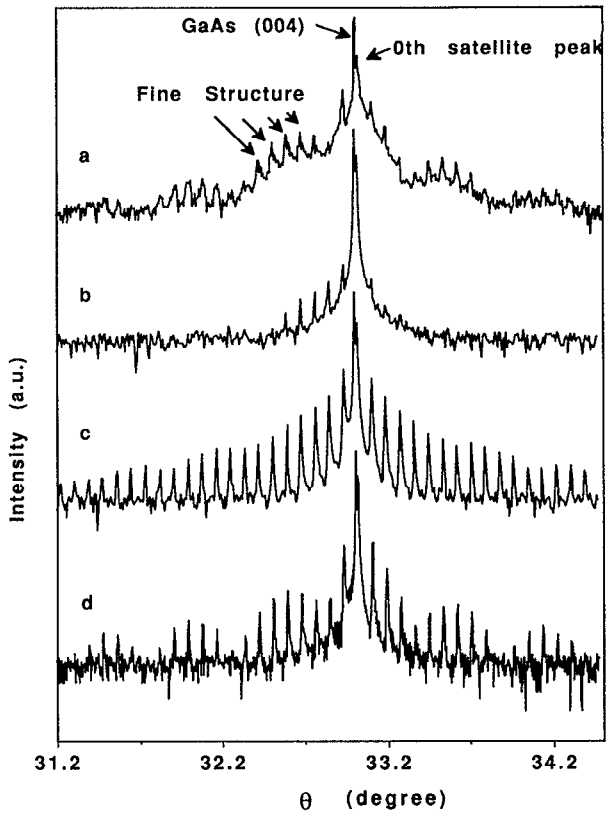

FIG. 5. (004) diffraction patterns of sample I; (a) measured pattern, (b) simulated pattern with the bilayer model, (c) simulated pattern with the trilayer model, and (d) simulated pattern with the four-layer model.

A progressive broadening of the superlattice satellites farther away from the 0th order satellite in (002) and (004) patterns is evidence for the existence of fluctuation in the superlattice period of sample I.

The simulations of the observed patterns are shown in Figs. 4 and 5 from 4(b) to 4(d) and from 5(b) to 5(d). They are performed as follows. The superlattice period is determined by fitting the observed superlattice satellites and the thickness of the well or barrier is decided by fitting the modulations of the superlattice satellites. It was observed that the same set of the simulation parameters can reproduce both the (002) and (004) patterns very well. This reveals that the influence of the substrate miscut and the tilt of the epilayer are well eliminated from the measured patterns. The alloy composition is determined by reproducing the observed mismatch. Simulation (b) in both Figs. 4 and 5 shows the simulated patterns with bilayer model, i.e., the GaAs well and GaInP barrier. All mismatch is accommodated by the GaInP barriers. Neither the symmetry and the modulation node positions in (002) pattern nor the intensities in (004) pattern is fitted. Apparently, there are extra layers. Simulation (c) in both Figs 4 and 5 show the simulated patterns with a trilayer model. A GaP layer at the GaInP/GaAs interface is added to the bilayer model. At this time, the mismatch is assumed to be accommodated by the GaP layer. There is no mismatch between the GaAs well and the GaInP barrier. The validity of this assumption will be discussed later. After adding a layer, the fitting of the (002) pattern improves a lot. But (004) is not simulated well for the modulation node positions and the relative intensities of the satellites. An interfacial layer may also exist in the GaAs/GaInP interface, which is another trilayer model. But there is no obvious difference from the interfacial layer at the GaInP/GaAs interface. Simulation (d) in both Figs. 4 and 5 show the simulated results with the four-layer model, i.e., in addition to the well and barrier layers, two interfacial layers are included in both GaInP/GaAs and GaAs/GaInP interfaces. The barrier is still assumed to be matched to the GaAs well. The agreement between the experiment and simulation by the four-layer model is satisfactory. The modulation node positions are reproduced well. Since no thickness fluctuation is considered in the simulation, the background is not simulated. The best fit layer thickness and mismatch are 4 Å and -1.2% at the GaAs/GaInP interface and 6 Å and -1.2% at the GaInP/GaAs interface, respectively; both interfacial layers are negatively strained. The simulated pattern is sensitive to the product of thicknesses and mismatches of the interfacial layers at both interfaces, which may change the node positions in

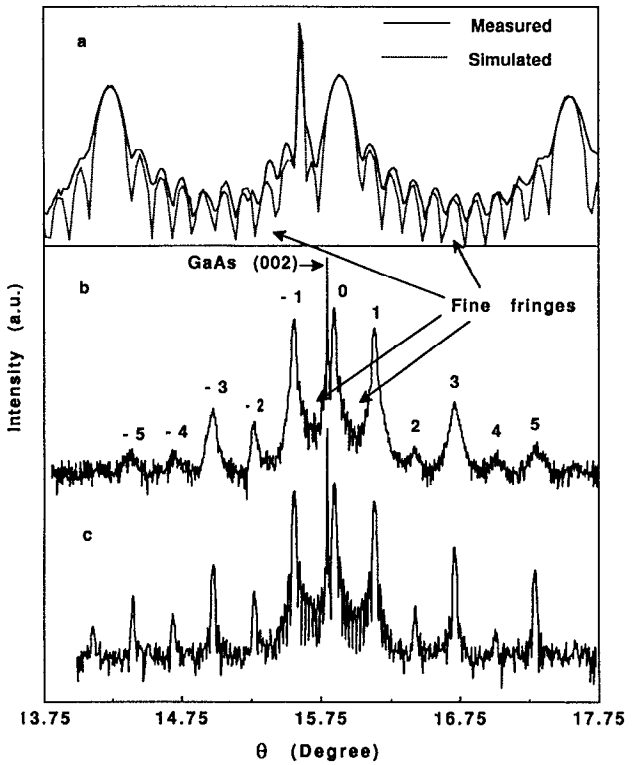

FIG. 6. (002) diffraction patterns of sample 2; (a) the magnification of both measured pattern and simulated patterns at the range of 15.75°–16.2° of θ, (b) measured pattern, and (c) simulated pattern with the four-layer model.

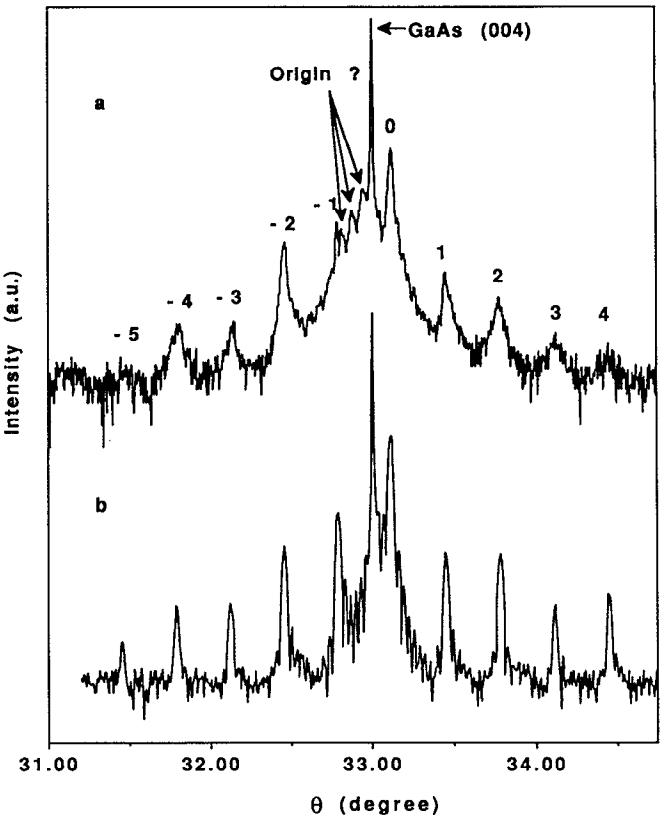

FIG. 7. (004) diffraction patterns of sample 2; (a) measured pattern and (b) simulated pattern with the four-layer model.

the simulated patterns. Although the thickness (or the mismatch) of the interfacial layer affects the simulated pattern, it cannot be decided precisely due to the lack of a strict criterion in the trial-and-error method.

The tilt of the epilayer measured from (115) is 24 s. This small tilt demonstrates that the density of mismatch dislocation is very low for sample I.

Figure 6(b) shows the (002) diffraction patterns of sample II. Except for the substrate peak, ten satellite peaks are observed in the diffraction pattern. The separation of these peaks indicates that the period of the superlattice is 157 ± 2 Å according to Eq. (3). The orders of the peaks is denoted in Fig. 6. Even order peaks are weak, which implies that the thickness of the well is very similar to that of the barrier (i.e., ≈ 79 Å). The clear fine fringes corresponding to a 1713 ± 10 Å layer are observed around the 0th order peak. The thickness of the layer is consistent with the total of ten periods of superlattice epilayers. Closer observation of the data shows that there is asymmetry in the diffraction pattern. Intensity of -2th satellite is much stronger than that of $+2$th satellite while $+3$th satellite is stronger than -3th order satellite. This suggests that there might be yet another thinner layer, in addition to the GaAs and GaInP layers in the superlattice unit cell. An averaged relaxed mismatch of -0.154% is derived from the separation of the substrate peak from the 0th order superlattice satellite in (002) diffraction patterns according to Eqs. (1) and (2).

Figure 7(a) shows the measured (004) diffraction pattern for sample II. Since the structure factor of GaAs (004) is not small anymore, the (004 diffraction pattern becomes quite complicated. Nine peaks attributed to the period of superlattice are observed. The separation of these peaks corresponds to a period of 158 ± 2 Å by Eq. (3), which is consistent with the result deduced from (002) diffraction pattern. The fine fringes corresponding to a larger thickness of 1622 ± 15 Å are visible. They are believed to be associated with the total superlattice. The weakening of the even order satellite peaks is not observed in the (004) pattern. This is because the modulation of the satellite peaks in the (004) pattern is decided by the harmonics from all layers in the superlattice unit cell rather than mostly due to only one layer in the superlattice unit cell as in the (002) pattern. An averaged relaxed mismatch of -0.153% is derived from the separation of the substrate peak from the 0th order superlattice satellite in the (004) diffraction pattern.

It is observed in both (002) and (004) diffraction patterns of sample II that the superlattice satellites are progressively broadened away from the 0th order peak. This broadening is evidence for a fluctuation in the superlattice period.

Gathering all of the above observations together as the input of the initial values, the same simulation procedure is performed for sample II. Similar to the simulation of sample 1, the bilayer model fails for both (002) and (004)

TABLE I. The structure parameters extracted from measurements and simulations. t and m are the thickness and the mismatch, respectively. Subscripts b, w-b, and b-w stand for the well, barrier, strained layer at the well/barrier interface, and strained layer at the barrier/well interface, respectively. m_a is the average relaxed mismatches of the samples.

Sample	t_{total} (Å)	t_{period} (Å)	m_a (%)	t_b (Å)	$t_{w\text{-}b}$ (Å)	$m_{w\text{-}b}$ (%)	$t_{b\text{-}w}$ (Å)	$m_{b\text{-}w}$ (%)
(002)	6519±304	612±4	−0.009[a]	...	...	...	...	...
I (004)	not observed	616±5	−0.019	...	...	...	...	...
Simul.	6661	614	−0.019	511	4	−1.17	6	−1.17
(002)	1713±10	157±2	−0.154	78.5	...	...	...	...
II (004)	1622±15	158±2	−0.153	79	...	...	...	...
Simul.	1659	158	−0.154	79	2	−2.43	8	−2.43

[a]This value is obtained by assuming the average of the +2th satellite and −2th satellite as the position of the 0th order superlattice satellite.

diffractions; the trilayer model works for (002), but fails to reproduce the weakening of odd order peaks observed in the (004) diffraction pattern; only the four-layer model works for both diffractions. The peaks intensity is sensitive to the product of mismatch and thickness of the interfacial strained layers. However, the product of mismatch and thickness of the interfacial strained layers deduced here is less reliable than that for sample I since there is no clear modulation of superlattice satellites for such a sample with thin superlattice period. Figure 6(a), which is the magnification of the spectra from 15.75° to 16.2° of θ, shows that remarkably close agreement is realized in the (002) pattern around the 0th order satellite. Even the fine fringes from the total thickness of the epilayer are reproduced well. The faster damping of the higher order satellites in the measured pattern than the simulated result shown in Fig. 6(c) may be caused by the interfacial roughness and crystal disorder in the sample, which is not considered in the simulation. The broadening of peaks is also not included in the simulations. The simulation of (004) in Fig. 7(b) indicates that the positions of the superlattice satellites are reproduced well and the fine fringe period of the total epilayer is fitted. But three peaks at the lower angular side of the substrate peaks are not shown in the simulated curve. These three peaks may be caused by a GaAs layer such that their trace would not show up in the (002) pattern. Considering that (004) diffraction is sensitive to every detail of the samples, the discrepancy observed is acceptable. The similar disagreement in (004) diffraction of GaInP/GaAs superlattices was also observed in other work.[4] However, the simulation does show that the even order peaks do not disappear for the equal thicknesses of the well and barrier at (004) diffraction.

The tilt of the epilayer is measured to be 167 s by measuring at (115) asymmetric geometry. This is much larger than that of sample I, so the density of mismatch dislocation for sample II is larger.

All our results are listed in Table I. It shows that the parameters measured from diffraction patterns are consistent. The measured and simulated superlattice period for sample II is very close to the real thickness (156 Å), which is measured by HRTEM (to be published elsewhere).

Table I shows that the superlattice period can be well measured from the diffraction pattern by Eq. (3). The reliable thickness of the barrier or well must be obtained by simulation. For a sample with thicker superlattice period as sample I, several modulations of superlattice satellites are observed. The obtained thickness of the barrier or well is more reliable. In comparison, for the sample with a thinner superlattice period such as sample II, no clear modulation of superlattice satellites is observed. It is a little bit difficult to get reliable well thickness. Fortunately, (002) diffraction of sample II gives us the information of the well thickness. The interface strains can only be decided by the simulation, but in our case, it seems the simulated patterns are only sensitive to the product of mismatch and thickness, which changes the node position of the modulation. The thickness or mismatch of the strained interfacial layer can be evaluated, but not very precisely because it is difficult to judge the best fit by only comparing the patterns by eye. The simulations of (002) and (004) diffractions also show that the fit to the (004) diffraction gives more reliable information on the sample structure. But, since the (002) diffraction gives stronger satellite peaks and more clear total thickness fringes, it is more reliable for the direct determination of the sample structure by using Eq. (3) without using simulations.

C. Origin of strained interfacial layers

The origin of the strained interfacial layers can be understood from Fig. 1. The strained layer at the GaInP/GaAs interface is caused by the purge of indium in order to remove its memory effect. Thus, an indium-poor GaInP grading layer definitely exists at the GaInP/GaAs interface. The strained layer at GaAs/GaInP is caused by the different traveling time in the gas lines for the phosphine and trimethalindium (TMI). Phosphine is in the low-pressure line. It takes fraction of a second to reach the sample surface. But TMI is in the line with atmospheric pressure. It takes seconds to get to the sample surface. Therefore, there is an indium-poor GaInP negative strained layer. This layer is about 1–2 monolayers thick.

It has been suggested that due to the atomic size difference between As and P, there is a positive strained monoatomic layer in the GaInAs/InP interface.[1] Our simulations show no positive strained layer at both interfaces. Thus the strained layers in our samples are more alike to

interfacial layers caused by the different pressures at gas lines, which has been suggested to cause a strained layer at the interface.[2]

D. The estimation of mismatch

In the above simulation, the GaInP barrier is assumed to be lattice matched to GaAs layers. This is reasonable when we combine the information of the two samples together. Since both samples are prepared in a similar condition, the larger mismatch for the thinner sample and smaller mismatch for the thicker sample indicate that the barriers are lattice matched very well to the GaAs wells and most of the mismatch is caused by the interfacial layers. A simple estimation of the mismatch of each layer in the superlattice unit cell can be made by assuming the same mismatch for the corresponding layers of the two samples and the same thickness of the interfacial layer for both samples. Also, the mismatches are assumed to be the same for both interfacial layers. As was known, the observed mismatch is related to the mismatch of each layer by $(m_b t_b + m_w t_w + m_i t_i)$/superlattice period=averaged mismatch observed, where m is mismatch and t is the thickness of the layer. Subscripts b, w, and i represent the barrier, well, and interfacial layer, respectively. Applying this equation to both samples, mismatches of 0.029% for the barrier and -2.6% for a total of 10 Å interfacial layers are obtained.

Since the barriers have a very small mismatch and the interfacial layers are thin and have a large mismatch, the interfacial layer is under strain. There is nearly no relaxation in the interfacial layers. This conjecture is consistent with the observation of a small tilt of epilayers, which is evident from the low mismatch dislocation density.

This estimation of mismatch is important because the simulations are valid for samples with no relaxation and the barrier is assumed to be lattice matched to the GaAs as a simplification in this work, which only is good for the barrier with very small mismatch.

V. CONCLUSION

Two ten-period superlattice samples were studied by HRXRD and the simulations by solving Tagaki–Taupin equations. Superlattice satellites are strong and well resolved in both samples. This indicates that the interface roughness and disorder of the samples are low for both samples. The strained interfacial layers at both GaAs/GaInP and GaInP/GaAs interfaces are identified from the simulations of the measured diffraction patterns. The purge of indium at the interface of GaInP/GaAs accounts for the strained layer at the GaInP/GaAs interface. Another strained layer at the GaAs/GaInP interface is attributed to the different pressure in the gas lines, which result in the different traveling time to the sample surface. Since the interface of the epilayer is very critical to the quality of the devices, the understanding of the interface strain is important to the improvement of the sample quality and the better understanding of the electronic properties of the samples. In addition, the influence of the miscut of the substrate to the measurement is discussed in the article. It shows that even though the miscut is small, the diffraction geometry is already an asymmetric one. More than 10% error in the superlattice period for a 2° miscut substrate can result when the consideration of a miscut substrate is considered as a symmetric geometry.

ACKNOWLEDGMENTS

The authors would like to thank Professor Jerry Cohen for his permanent support and encouragement. The authors also acknowledge the support of Dr. Gail Brown and are grateful for the funding from KOPIN Corporation and U.S. Air Force.

[1] J. M. Vandenberg, A. T. Macrander, R. A. Hamm, and M. B. Panish, Phys. Rev. B **44**, 3991 (1991).
[2] M. H. Lyons, J. Cryst. Growth **96**, 339 (1989).
[3] R. Zaus, M. Schuster, H. Gobel, and J. P. Reithmaier, Appl. Surf. Sci. **50**, 92 (1991).
[4] N. Herres, G. Bender, and G. Neumann, Appl. Surf. Sci. **50**, 97 (1991).
[5] M. Razeghi, P. Maurel, F. Omnes, M. Defour, C. Boothroyd, W. M. Stobbs, and M. Kelly, J. Appl. Phys. **63**, 4511 (1988).
[6] M. Razeghi, P. Maurel, F. Omnes, S. Ben Armor, L. Dmowski, and J. C. Portal, Appl. Phys. Lett. **48**, 19 (1986).
[7] F. Omnes and M. Razeghi, Appl. Phys. Lett. **59**, 1034 (1991).
[8] J. S. Nelson, S. R. Kurtz, L. R. Dawson, and J. A. Lott, Appl. Phys. Lett. **57**, 578 (1990).
[9] P. F. Fewster and C. J. Curling, J. Appl. Phys. **62**, 4154 (1987).
[10] S. Takagi, Acta. Crystallogr. **15**, 1311 (1962); J. Phys. Soc. Jpn. **26**, 1239 (1969).
[11] D. Taupin, Bull. Soc. Fran. Miner. Cryst. **87**, 469 (1964).
[12] M. Razeghi, M. Defour, F. Omnes, M. Dobers, J. P. Vieren, and Y. Guldner, Appl. Phys. Lett. **55**, 457 (1989).
[13] M. Razeghi, F. Omnes, J. Nagle, M. Defour, O. Acher, and P. Bove, Appl. Phys. Lett. **55**, 1677 (1989).
[14] W. J. Bartels, J. Vac. Sci. Technol. B **1**, 338 (1983).
[15] M. A. G. Halliwell and M. H. Lyons, J. Cryst. Growth **68**, 523 (1984).